



## Photovoltaic and Electrical Properties of Al/ Ruthenium (II)-complex / p-Si Photodiode

Hülya DOĞAN<sup>1</sup>, İkrâm ORAK<sup>2</sup>, Nezir YILDIRIM<sup>2,3</sup>

<sup>1</sup>Cumhuriyet University, Faculty of Engineering, Department of Electric and Electronics Engineering, 58140 Sivas, Turkey

<sup>2</sup>Bingöl University, Vocational School of Health Services, 12000 Bingöl, Turkey

<sup>3</sup>Bingöl University, Faculty of Sciences and Arts, Department of Physics, 12000 Bingöl, Turkey

Received: 10.03.2017; Accepted: 04.04.2017

**Abstract.** This study is about the deposition of tris (2,2'-bipyridine) Ruthenium(II)-complex thin film on p-type crystalline silicon (Si) by spin coating method (Al/Ru(II)/p-Si). The characteristics parameters were evaluated from the current-voltage ( $I-V$ ) under dark and illumination at room temperature. First, the optical properties of the organic thin film were determined from its optical absorption spectrum, and its band gap was found to be 2.74 eV. Then, the electrical parameters of the Al/Ru(II)/p-Si photodiode, such as the ideality factor ( $n$ ), barrier height ( $\Phi_b^{I-V}$ ), diffusion potential, barrier height ( $\Phi_b^{C-V}$ ) and carrier concentration ( $N_a$ ) were calculated from the  $I-V$  and  $C-V$  measurement at room temperature. Both measurements barrier height values were compared. Cheung method was used to determine the series resistance ( $R_s$ ), barrier height and ideality factor, under dark and 100 mW/cm<sup>2</sup> illumination conditions. The photovoltaic parameters of the studied device were investigated under illumination conditions. The open-circuit voltage and short circuit current values for the Al/Ru(II)/p-Si were found to be  $439.9 \times 10^{-3}$  V and  $36.6 \times 10^{-6}$  A respectively. Ruthenium(II) complex positively influences the photovoltaic performance. These results reveal that the Al/Ru(II)/p-Si built can be used as a photodiode in photovoltaic and photodetector applications.

**Keywords:** Ruthenium(II)-complex, photodiodes, illumination effect on electrical characteristics, series and shunt resistances.

## Al/Ruthenium(II) complex/ p-Si Fotodiyotun Fotovoltaik ve Elektriksel Özellikleri

**Özet.** Bu çalışma, p-Si kristali üzerine tris (2,2'-bipyridine) Ruthenium(II)-complex ince filmin döndürme kaplama yöntemi ile (Al/Ru(II)/p-Si) yapısının oluşturulması ile ilgilidir. Karakteristik parametreler oda sıcaklığında karanlık ve aydınlatma durumundaki akım-gerilim ( $I-V$ ) eğrilerinden belirlendi. İlk olarak organik ince filmin optiksel özellikleri, soğurma spektrumu kullanılarak, bant aralığı 2.74 eV olarak bulundu. Ondan sonra Al/Ru(II)/p-Si fotodiyotunun, idealite faktörü ( $n$ ), engel yüksekliği ( $\Phi_b^{I-V}$ ), difüzyon potansiyeli, engel yüksekliği ( $\Phi_b^{C-V}$ ) ve taşıyıcı konsantrasyonu ( $N_a$ ) gibi elektriksel parametreler, oda sıcaklığında ( $I-V$ ) ve ( $C-V$ ) ölçümlerinden hesaplandı. Her iki engel yüksekliği değeri birbirleri ile karşılaştırıldı. Cheung metodu kullanılarak karanlık ve 100 mW/cm<sup>2</sup> aydınlatma durumu altında seri direnç ( $R_s$ ), engel yüksekliği ve idealite faktörü belirlendi. Devrenin fotovoltaik parametreleri aydınlatma durumunda incelendi. Al/Ru(II)/p-Si için açık devre voltajı ve kısa devre akımı sırasıyla  $439.9 \times 10^{-3}$  V ve  $36.6 \times 10^{-6}$  A olarak bulundu. Ruthenium (II) complex, fotovoltaik performansı pozitif olarak etkilemiştir. Bu sonuçlar Al/Ru(II)/p-Si yapısının fotovoltaik ve fotodedyör uygulamalarında bir fotodiyot olarak kullanılabilceğini ortaya çıkarmıştır.

**Anahtar Kelimeler:** Ruthenium (II) complex, fotodiyot, elektriksel karakteristiklere aydınlatma etkisi, seri ve şönt direnci.

\* Corresponding author. Email address: hdogan@cumhuriyet.edu.tr

## 1. INTRODUCTION

Photodiodes are semiconductor optoelectronic devices that transform light into current and are for to perform in reverse bias. Components of a photodiode are a semiconductor material and some junctions such as metal-semiconductor (Schottky), p-n, and p-i-n. Recent studies on electronic and optoelectronic devices dwells more on organometallic compounds. The thermal stability, photochemical, photophysical and electrochemistry properties of Ruthenium(II) complexes have been broadly studied [1]. These features have driven the development of several applications of ruthenium (II) complexes (e.g. artificial photosynthetic frameworks [2], sensors [3], and catalysis [4]). Of these applications, dye-sensitized solar cells (DSCs) have caught significant attention as an alternative to conventional silicon photovoltaic devices [5,6]. Namely, O'Regan and Gratzel [7] reported a low cost, high efficiency dye-sensitized solar cell using a Ru (II) complex. A number of solar cells and Schottky diodes have been fabricated using phthalocyanine complexes [8,9]. Ocak et al. [ 10] have shown the possibility of Schottky diodes formation by new, synthesized Mn hexaamide (MnHA) organometallic complex. So, both the synthesis of new organometallic complexes and the use of these in the fabrication of devices are of great interest.

Electronic applications are now using metal complexes for their crucial electrical and optical properties. Electronic, optical and chemical properties of Ru(II) complexes make them indispensable components. Tataroglu et al. [11] studied, using drop casting technique, the preparation of Au/Ruthenium(II) complex/n-Si photodiode. After these photo response measurements, they [11] found that the photodiode demonstrated itself as photo conductor and a photo capacitant. Soyulu et al. [12] have produced Ruthenium (II) complex with polydentate pyridine on the surface of a Si substrate by spin-coating method. They [12] revealed those photovoltaic properties using illumination –dependent I-V measurements. Orak et al. [13] produced organic-inorganic heterojunction and researched the effect of thickness of the organic layer on the electrical and photovoltaic performance. Aydogan et al. [14] produced a polyaniline/p-Si/Al MIS device by forming a polyaniline layer on Si, through the electrochemical polymerization technique. They carried out capacitance-voltage-frequency measurements as a function of temperature.

Studies indicate that the barrier height of an inorganic semiconductor can be either increased or decreased using an organic thin layer [15-18]. The electrical and photoelectrical characteristics of metal-semiconductor (MS) devices with a thin organic interfacial layer have been studied for photovoltaic cells, photodiodes, and Schottky diodes [19-22]. Güllü et al. fabricated an Al/Orange G/p- Si device with a barrier height (0.77 eV) greater than that of a conventional Al/p-Si contact (0.50 eV) [23]. Temirci and Çakar have found a barrier height of 0.78 eV and an ideality factor of 1.54 for a Cu/rhodamine 101/p-Si/Al diode [24]. This barrier height was higher than that of a conventional Cu/p-Si contact. Ozaydın et al. [25] fabricated an Au/Cu(II) complex/n-Si structure by forming a thin Cu(II) complex layer on n-Si wafers by spin coating. They [25] investigated the electrical parameters of Au/Cu(II)complex/n-Si Schottky diode using forward-bias current–voltage(I–V) measurements and compared the parameters to those for a conventional Au/n-Si diode.

In this study, the electrical (I-V and C-V) and photovoltaic characteristics of an Al/Ru(II)/p-Si photodiode were determined under dark conditions as well as under 100mW/cm<sup>2</sup> illumination condition. For this, Ruthenium(II) complex with a formula of (C<sub>30</sub>H<sub>24</sub>F<sub>12</sub>N<sub>6</sub>P<sub>2</sub>Ru) was used. The morphological properties of the Ru(II) complex were determined with the AFM method. In addition, the band gap of this complex was determined with a measurement of optical absorption.

## 2. EXPERIMENTAL DETAILS

In this study, p-type silicon semiconductor with an orientation of (100), a thickness of 525  $\mu\text{m}$ , and a specific resistance in the 1-10  $\Omega\cdot\text{cm}$  range was used. For the chemical cleaning of the p-Si wafer, the RCA cleaning method was applied (i.e. first boiling in  $\text{H}_2\text{SO}_4+\text{H}_2\text{O}_2$  and then in  $\text{HCl}+\text{H}_2\text{O}_2+6\text{H}_2\text{O}$  for 10 min at 60  $^\circ\text{C}$ , in each step) [26]. After the cleaning process, aluminum metal of 100 nm thickness was formed on the matt surface for ohmic contact process, using the thermal evaporation (deposition) method. The sample was annealed for 3 minutes in an oven preheated to 450  $^\circ\text{C}$  under nitrogen gas and the ohmic contact process was completed. After the ohmic contact process, tris(2,2'-bipyridine)ruthenium(II) organometallic complex with a molecular formula of  $(\text{C}_{30}\text{H}_{24}\text{F}_{12}\text{N}_6\text{P}_2\text{Ru})$  (for the complex structure see Figure 1.(a)), obtained Sigma Aldrich, was used as an intermediate layer. For this process, Ru (II) (0.01 M) solution was prepared with ethanol. The Ru(II) was directly formed by casting 5 mL of the 0.001 M Ru(II) solution in alcohol on the front surface of the p-Si substrate and then spin coating the solution onto the Si substrate, which was rotated at 500 rpm/min for 30 s and then dried for 60 min at room temperature in order to remove the solvent. After the Ru(II) complex was formed, using aluminum metal thickness control monitor, Al/Ru(II)complex/p-Si/Al of 100 nm thickness was formed with the thermal evaporation method. The radius of the discs shown in Figure 1(b) is 1 mm and their area is  $7.85 \times 10^{-3} \text{ cm}^2$ . All evaporation processes have been carried out at a pressure of  $4 \times 10^{-6}$  Torr and under vacuum. Photovoltaic measurements were carried out at room temperature with Keithley 2400 and COINC-16S-150-002, using solar simulator. Keithley 4200 SCS was used for the capacitance-voltage measurements of the samples. The optical characterization of the Ru(II) complex was carried out with a Shimadzu UV-VIS spectrophotometer and for determining surface morphology of the sample AFM (Atomic Force Microscopy) was used.

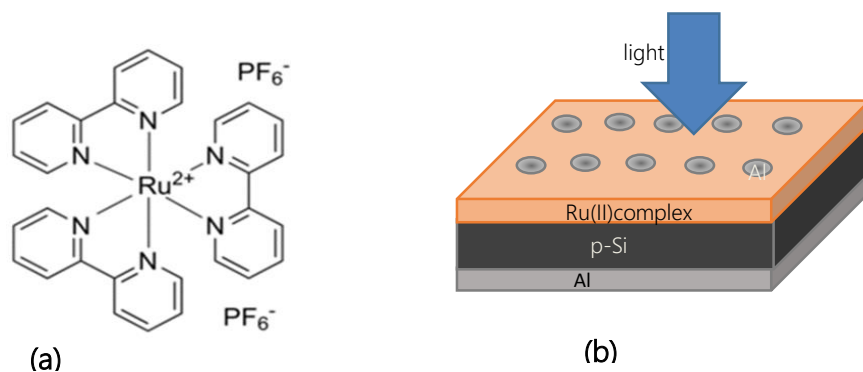


**Figure 1.** (a) Molecular structure of the Ruthenium(II) complex ( $\text{C}_{30}\text{H}_{24}\text{F}_{12}\text{N}_6\text{P}_2\text{Ru}$ ); (b) device structure of Al/Ru(II)/p-Si

## 3- RESULTS AND DISCUSSION

### 3.1 Optical and structural properties of Ru(II) complex thin film

The morphological properties of the Ru(II) complex that was coated on the p-Si substrate determined with Atomic Force Microscopy (AFM). As can be seen in Figure 2, the Ru(II) complex was distributed on the semiconductor surface homogeneously.

## Photovoltaic and Electrical Properties of Al/ Ruthenium (II)

The optical properties of the Ru(II) complex were analyzed with a UV/VIS spectrophotometer at room temperature. The absorbance spectrum of the Ru(II) complex is given in Figure 3 and its transmittance spectrum is shown in the small insert in the figure. The highest absorption intensity was observed around 454 nm. A peak was observed around 454 nm in the absorption spectrum and the absorption spectrum remained stable at the 570-750 nm wavelength range (see inset in Fig. 3).

The optical bandwidth ( $E_g$ ) of the Ru(II) complex is obtained with the following formula [27,28]:

$$\alpha h\nu = B(h\nu - E_g)^m \quad (1)$$

Here  $\alpha$  is the absorption coefficient,  $B$  is a constant,  $h$  is the Planck's constant ( $h=6.626 \times 10^{-34}$  J.s), and  $m$  is a constant, which takes the value of 1/2 for a direct bandwidth and 2 for an indirect bandwidth. Both of the  $(\alpha h\nu)^2 - h\nu$  and  $(\alpha h\nu)^{1/2} - h\nu$  (insert) plots are given together in Figure 4. The direct and indirect bandgap ( $E_g$ ) of the Ru(II) complex were obtained as 2.4 and 2.02 eV, respectively, from the intercept of the extrapolated linear parts of the  $(\alpha h\nu)^2 - h\nu$  and  $(\alpha h\nu)^{1/2} - h\nu$  (insert) plots on the photon energy axis.

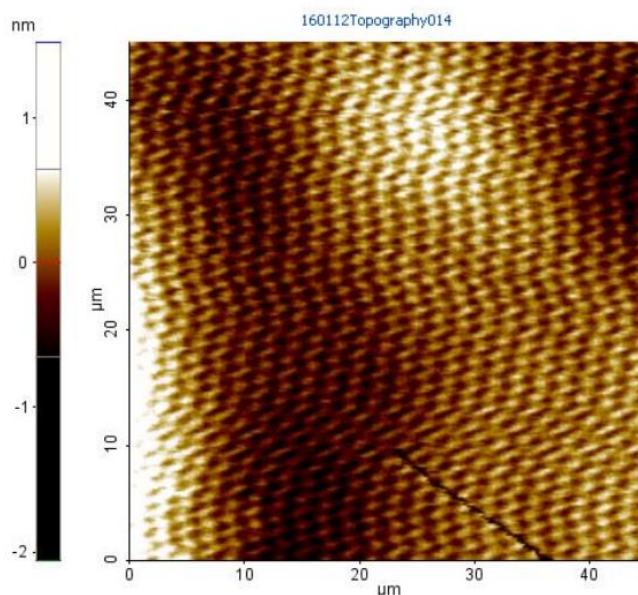


**Figure 2.** The 2D AFM images of Ru(II)-complex structure.

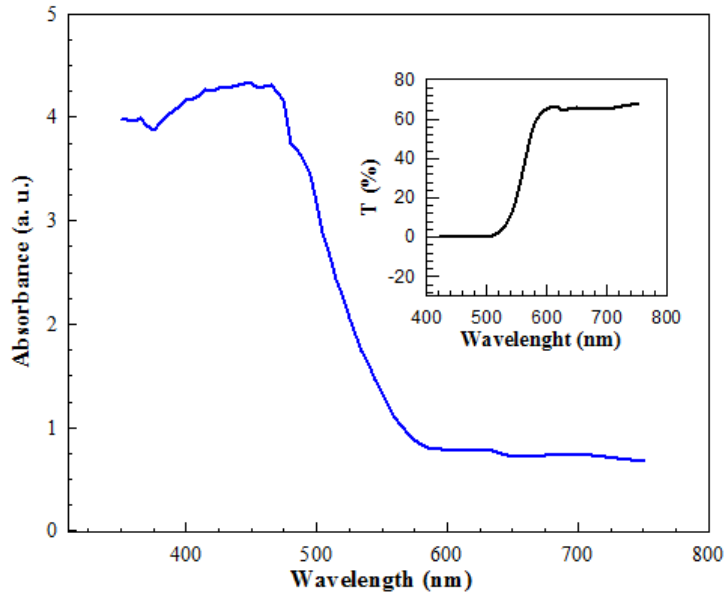


Figure 3. The absorbance spectra of the Ru(II)-complex film (inset shows the transmittance spectra).

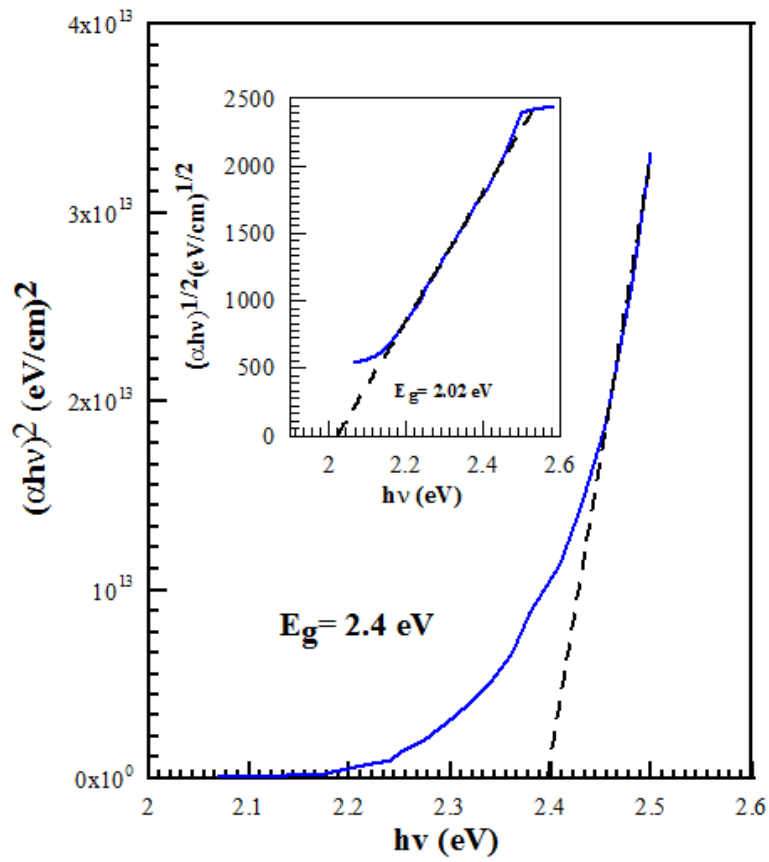


Figure 4. Plot of  $(\alpha hv)^2$  versus  $h\nu$  of Ru(II)-complex film (inset show  $(\alpha hv)^{1/2}$  versus  $h\nu$ ).

### 3-2. Electrical and photoelectrical properties of Al/Ru(II) complex/p-Si

A solar simulator was used for the photoelectrical characterization of the Al/Ru(II)/p-Si structures. Current-voltage (I-V) measurements were carried out with a solar simulator with a AM1.5 global filter, under illumination intensity of 100 mW/cm<sup>2</sup> in order to analyze material response to light. The plot obtained for the Al/Ru(II)/p-Si in these measurements is shown in Figure 5. It can be seen in the plot that the diode gives response under illumination. The sensitivity of the Al/Ru(II)/p-Si structure to light was obtained by taking the ratio of the current value obtained at -2 V and 100 mW/cm<sup>2</sup> light intensity to its current value obtained under dark conditions ( $I_{\text{illumination}}/I_{\text{dark}}$ ) and was found as  $2.48 \times 10^4$ .

In order to analyze the I-V characteristics of the Al/Ru(II)/p-Si, thermionic emission (TE) model was used and this model can be expressed as follows [29]:

$$I = I_0 \exp\left(\frac{qV}{nkT} - 1\right) \quad (2)$$

where  $I_0$  is the saturation current defined by

$$I_0 = AA^*T^2 \exp\left(\frac{-q\Phi_{b0}}{kT}\right) \quad (3)$$

$\Phi_{b0}$  is the zero bias apparent barrier height (BH),  $q$  is the electron charge,  $k$  is the Boltzmann constant,  $T$  is the absolute temperature,  $V$  is the forward-bias voltage,  $A$  is the effective diode area,  $A^*$  is the Richardson constant of  $32 \text{ A cm}^{-2}\text{K}^{-2}$  for  $p$ -type Si. In order to calculate the ideality factors ( $n$ ) of the diodes, if the natural logarithm of the both sides of the (2) equalities is taken and its derivative is taken with respect to  $V$ , the following relation is obtained:

$$n = \frac{q}{kT} \left( \frac{dV}{d \ln I} \right) \quad (4)$$

The ideality factor is a dimensionless parameter that gives an idea whether the diode is ideal or not. If  $n$  varies between 1 and 2, the tunneling current mechanism is dominant. If  $n = 2$ , the generation recombination current mechanism is the dominant mechanism. If  $n > 2$ , then the leakage current mechanism is dominant [30].  $\Phi_{b0}$  is calculated by the following formula:

$$\Phi_b = \frac{kT}{q} \ln\left(\frac{AA^*T^2}{I_0}\right) \quad (5)$$

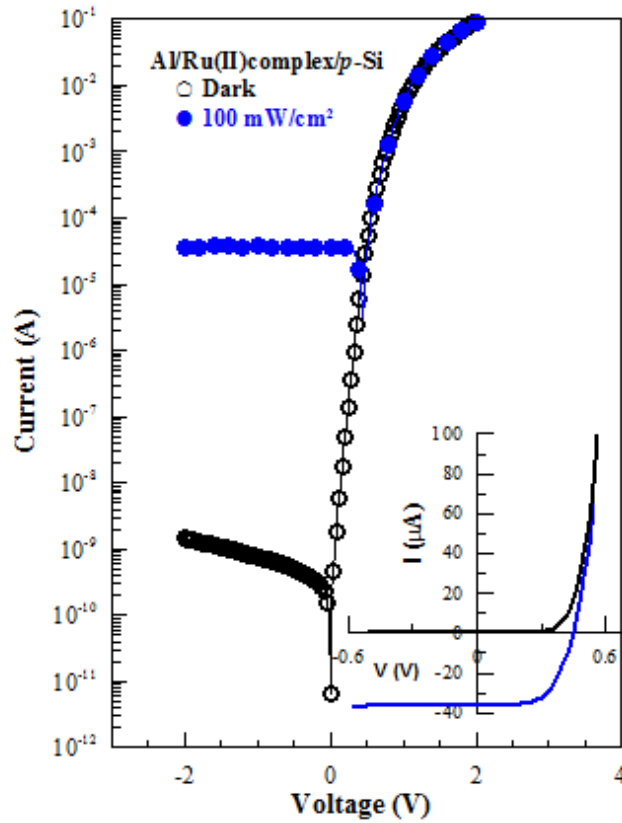


**Figure 5.** Forward and reverse bias ln-I-V plot of the Al/Ru(II)/p-Si structure in dark and under 100 mW/cm<sup>2</sup> illumination level.

The barrier heights and the ideality factors obtained from Figure 5 for the Al/Ru(II)complex/p-Si photodiode under dark and under 100 mW/cm<sup>2</sup> illumination conditions at room temperature are given in Table 1. As can be seen in Table 1, the n ideality factor and the barrier height are 1.52 and 0.82 eV, respectively under dark and 3.22 and 0.46 eV, respectively under 100 mW/cm<sup>2</sup> illumination. An ideality factor higher than 1 was obtained. This result can be explained with the presence of barrier inhomogeneities, interface states, and series resistance [31-33].

**Table 1.** The parameters obtained from current-voltage (I-V) characteristics of the Al/Ru(II)/p-Si structure in dark and under 100 mW/cm<sup>2</sup>.

Sample	I-V characteristic				Cheung-Cheung			
					Cheung		H function	
	n	$\Phi_{B0}$ (eV)	$R_s$ ( $\Omega$ )	$R_{sh}$ ( $\Omega$ )	$R_s$ ( $\Omega$ )	n	$R_s$ ( $\Omega$ )	$\Phi_{B0}$ (eV)
Al/Ru(II)/p-Si dark	1.52	0.81	21.67	$1.4 \times 10^9$	7.21	3.85	9.73	0.82
Al/Ru(II)/p-Si light	3.22	0.46	21.69	$5.4 \times 10^4$	6.74	4.86	9.54	0.39

The reason for obtaining an ideality factor higher than one is the series resistance effect ( $R_s$ ), which leads to the parts of the forward bias current-voltage curves that correspond to high voltages bend downwards. Two parameters are important in the linear and non-linear parts of the forward bias I-V plots [34]. These are n and  $\Phi_{b0}$ . The  $R_s$ , n, and  $\Phi_{b0}$  were determined with the method of Cheung and Cheung [35]. The Cheung function is expressed as

$$\frac{dV}{d(\ln I)} = IR_s + n \left( \frac{kT}{q} \right) \quad (6)$$

and

$$H(I) = V - \frac{nkT}{q} \ln \left( \frac{I}{AA^*T^2} \right) = IR_s + n\Phi_b \quad (7)$$

The term  $IR_s$  is the voltage drop across series resistance of diode. The  $dV/d(\ln(I))$ - $I$  and  $H(I)$ - $I$  plots of the Cheung functions for the Al/Ru(II)complex/p-Si diodes for the dark condition are given in Figure 6. The  $dV/d\ln(I)$ - $I$  plot given with Equation (6) is linear. Therefore the ideality factor was obtained from the intercept of this line on the vertical axis when  $I=0$  and the serial resistance was obtained from the slope of this line. The  $H(I)$ - $I$  plot given with Equation (7) similarly is linear. Using the ideality factor obtained from Equation (6), the diode's barrier height and the serial resistance, which is the resistance of the neutral region, was found. The serial resistance, barrier height, and ideality factor values for the dark and illumination conditions ( $100 \text{ mW/cm}^2$ ), obtained from the Cheung functions can be seen in Table 1. As can be seen in Table 1, the serial resistance values obtained from the  $dV/d\ln(I)$ - $I$  and  $H(I)$ - $I$  plots are in harmony with each other.

In addition, the serial resistance ( $R_s$ ), which is the resistance of the neutral region of the Al/Ru(II)complex/p-Si photodiode, the shunt resistance ( $R_{sh}$ ), which arises from the semiconductor-electrode interface properties, were calculated from the Ohm's Law using the  $I$ - $V$  data [36]. The shunt resistance and the serial resistance affect the current-voltage characteristics of the diode [37]. For an ideal diode, the shunt resistance has to be large and the serial resistance should be small [38]. The connection resistance of the photodiode is  $R_i$  ( $R_i = dV/dI$ ). As can be seen in Figure 7, the  $R_s$  and  $R_{sh}$  values were obtained for dark and  $100 \text{ mW/cm}^2$  illumination conditions from the  $R_i$ - $V$  plots (in addition, see Table 1). As can be seen from Table 1, there is a very large difference between  $R_s$  and  $R_{sh}$ . This shows that the Al/Ru(II)complex/p-Si structure is suitable for potential applications.

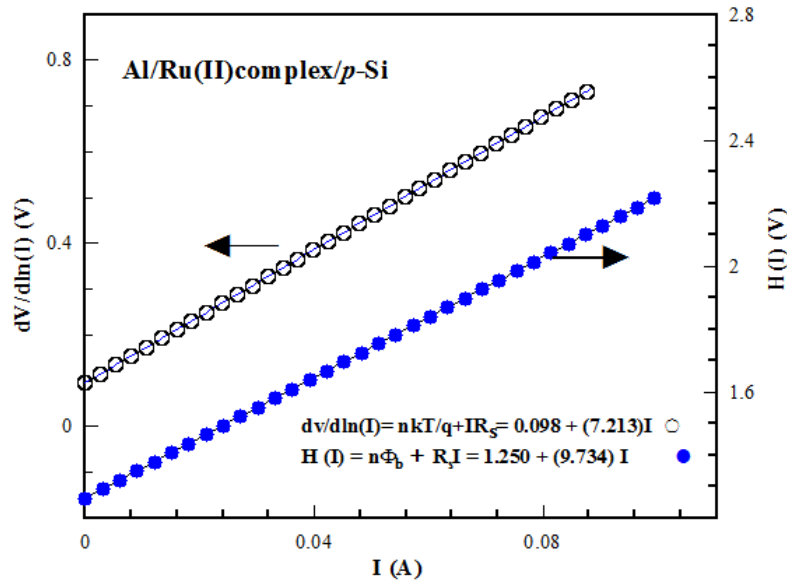


**Figure 6.** Experimental  $dV/d\ln(I)$  vs.  $I$  and (b)  $H(I)$  vs.  $I$  plots of Al/Ru(II)/p-Si in dark.

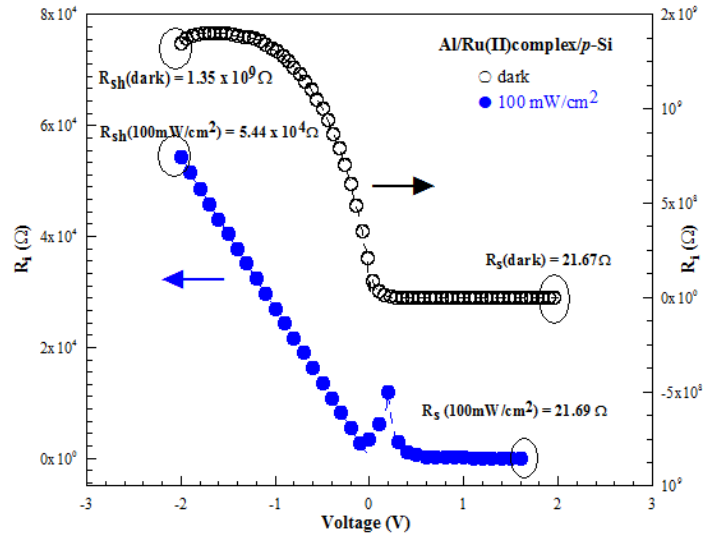


**Figure 7.** The structure resistance of Al/Ru(II)/*p*-Si structure calculated from I-V data in dark and under 100 mW/cm<sup>2</sup>.

Photovoltaic parameters of the Al/Ru(II)complex/*p*-Si structure, such as the open-circuit voltage, short-circuit current, fill factor and power conversion efficiency ( $\eta_p$ ) were calculated. In the current-voltage characteristic of the diode under illumination, the value of the curve's intercept on the voltage axis is called the open-circuit voltage  $V_{oc}$  and is determined when the current is zero. The short-circuit current ( $I_{sc}$ ), is the output current under illumination and is the current when the applied voltage and the resistance values ( $R_s$  and  $R_{sh}$ ) are zero. This current is proportional to the incoming number of photons and the illumination intensity. The open-circuit voltage and the short-circuit current are the highest voltage and current values, respectively (see Figure 8). As can be seen in Table 2, the  $V_{oc}$  and  $I_{sc}$  values of the Al/ Ru(II)complex /*p*-Si structure were calculated as  $439.9 \times 10^{-3}$  V and  $36.6 \times 10^{-6}$  A, respectively. Other photovoltaic parameters are the fill factor (FF) and the power conversion efficiency ( $\eta_p$ ). FF and  $\eta_p$  can be calculated from the J-V measurements given in Figure 8. FF can be written as [39]:

**Table 2.** Photoelectrical parameters of Al/Ru(II)/*p*-Si structure under illumination 100 mW/cm<sup>2</sup> light.

Sample	$J_m (10^{-3})$ A/m <sup>2</sup>	$V_m (10^{-3})$ V	$I_{sc} (10^{-6})$ A	$V_{oc} (10^{-3})$ V	FF (%)	$\eta_p$ (%)
Al/Ru(II)/ <i>p</i> -Si	3.9	319.9	36.6	439.9	60.8	1.25

$$FF = \frac{J_m V_m}{J_{sc} V_{oc}} \tag{8}$$

$J_m V_m$  is the maximum power point and FF was calculated as 62.9% for the Al/Ru(II)complex/*p*-Si. The power conversion efficiency,  $\eta_p$ , is [40]:

$$\eta_p = \frac{J_m V_m}{P_0} \tag{9}$$

where  $P_0$  is the light density, which is approximately  $100 \text{ mW/cm}^2$ . The power conversion efficiency ( $\eta_p$ ) was found to be 1.25% (see Figure 8 and Table 2).

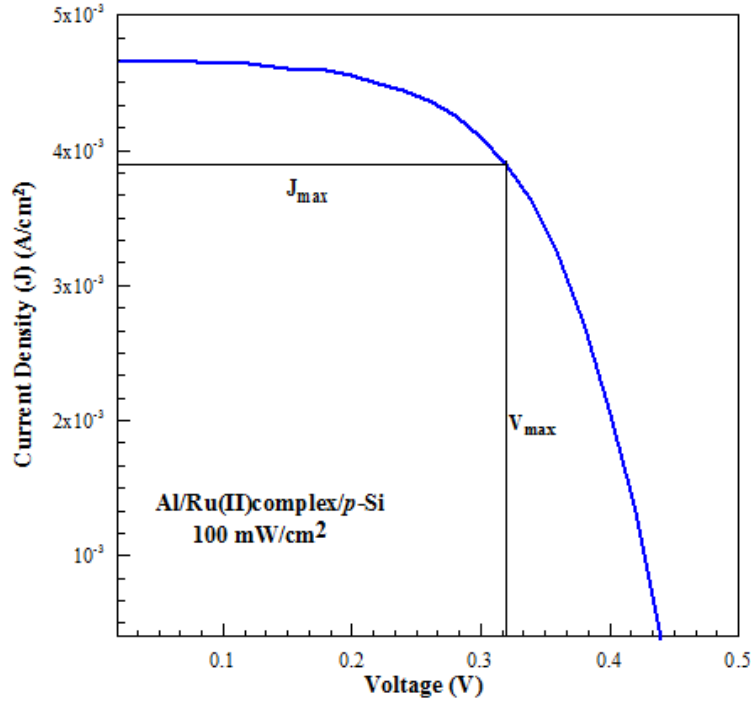


**Figure 8.** Current density-voltage plot of under illuminations for calculated FF and  $\eta_p$  of Al/Ru(II)/p-Si structure.

Another method that is used to determine the barrier height is the C-V measurement method. The C-V and  $C^{-2}$ -V plots of the Al/Ru(II)complex/p-Si structure at 500 kHz frequency, room temperature and under dark are given in Figure 9. The capacitance of the space charge region of a metal/semiconductor gives important information about the formation of the interface. If the capacitance is measured based on the reverse bias voltage, the barrier height of the rectifier contact, the carrier concentration in the semiconductor, the diffusion potential, and the Fermi energy level can be calculated [41].

$$\frac{1}{C^2} = \frac{2(V_d + V)}{A^2 \epsilon_s \epsilon_0 e N_a} \quad (10)$$

Here  $\epsilon_s$  is the semiconductor dielectric constant (for Si  $\epsilon_s = 11.8$ );  $\epsilon_0 = 8.85 \times 10^{-14} \text{ F/cm}$  is the vacuum permittivity;  $e$  is electronic charge ( $e = 1.6 \times 10^{-19} \text{ C}$ );  $V_d$  is the diffusion potential;  $k$  is the Boltzmann constant;  $N_a$  is the ionized acceptor concentration;  $T$  is the ambient temperature in Kelvin (K), and  $A$  is the effective area of the diode ( $A = 0.00785 \text{ cm}^2$ ). The barrier height can be calculated by the following relation:

$$\Phi_b = \frac{V_d}{n} + V_p \quad (11)$$

Here,  $V_p$  is the potential difference between the top of the valence band of the neutral part of p-Si and the fermi level, and is expressed as follows:

$$V_p = \frac{kT}{e} \ln \left( \frac{N_v}{N_a} \right) \quad (12)$$

Here,  $N_v$  is the effective density of Si's valance band and its value was taken as  $1.04 \times 10^{-4} \text{ cm}^{-2}$ . In Figure 9, the  $C^{-2}$ -V characteristic of the Al/Ru(II)complex/p-Si diode under 500 kHz frequency and dark is shown. With a linear fit suitable for this graph and for  $C^{-2}=0$ ,  $V_d=V$ . Therefore the diffusion potential is found as ( $V_d=0.497 \text{ V}$ ). Using Equations 11 and 12, the barrier height was found as ( $\Phi_b=0.84 \text{ eV}$ ). This value of the barrier height which was obtained under dark from the C-V measurements, is higher than the barrier height value ( $\Phi_b=0.81 \text{ eV}$ ) obtained from the I-V measurements under dark.

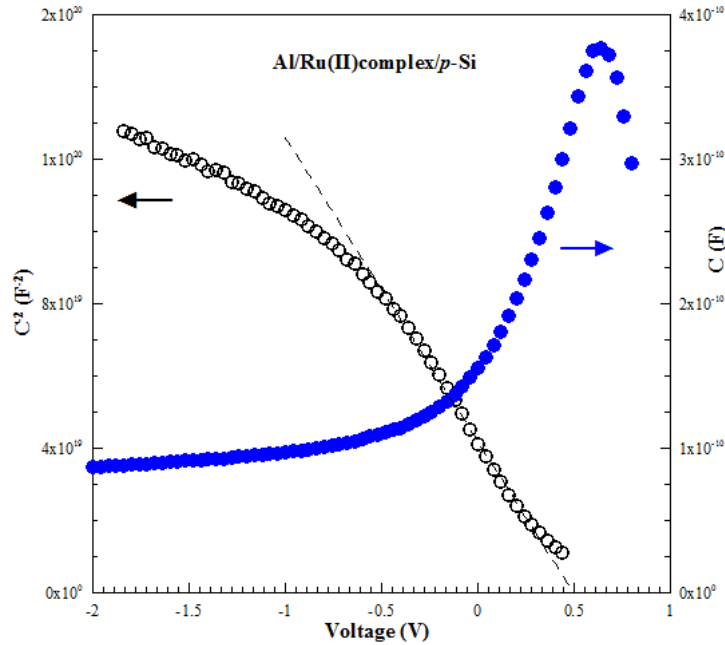


**Figure 9.** The capacitance-voltage and the reverse bias  $C^{-2}$ -V plot at 500 kHz for the Al/Ru(II)complex/p-Si structure.

#### 4. CONCLUSION

Al/Ru(II)/p-Si heterojunction device has been fabricated by thermal evaporation and spin coating technique. The electrical and photoelectrical characterizations of the fabricated devices were investigated by using I-V and C-V measurements at room temperature. I-V measurements; the barrier height, ideality factor, series resistance, and shunt resistance of the Al/Ru(II)/p-Si structure was calculated for dark and  $100 \text{ mW/cm}^2$  illumination conditions. In addition, from the C-V measurements, the barrier height, diffusion potential, and the carrier concentration was obtained for the dark condition. From the results it was deduced that the diode had a good rectifier property and photodiode property. Using optical absorption spectroscopy, the direct and indirect optical bandwidths of the Ru(II) complex film were found as  $2.74 \text{ eV}$  and  $2.02 \text{ eV}$ , respectively. The photovoltaic performances of the junction devices were determined using an open circuit voltage ( $V_{oc}$ ), short circuit current ( $I_{sc}$ ), fill factor (FF) and power conversion efficiency ( $\eta_p$ ) at  $100 \text{ mW/cm}^2$  and room temperature. The values were found to be  $439.9 \times 10^{-3} \text{ V}$ ,  $36.6 \times 10^{-6} \text{ A}$ ,  $60.8\%$ , and  $1.25\%$  for Al/Ru(II)/p-Si, respectively. Thus, Ru(II) complex thin film deposited on p-Si substrate can be used for some optoelectronic applications and solar cells.

## REFERENCES

- [1]. D.L. Ashford, M.K. Brennaman, R.J. Brown, S. Keinan, J.J. Concepcion, J.M. Papanikolas, J.L. Templeton, T.J. Meyer, *Inorg. Chem.* 54 (2015) 460–469.
- [2]. J.J. Concepcion, J.W. Jurss, M.K. Brennaman, P.G. Hoertz, A.O.T. Patrocinio, N.Y. Murakami Iha, J.L. Templeton, T.J. Meyer, *Acc. Chem. Res.* 42 (2009) 1954–1965.
- [3]. P.D. Beer, J. Cadman, *Coord. Chem. Rev.* 205 (2000) 131–155.
- [4]. R. Argazzi, N.Y. Murakami Iha, H. Zabri, F. Odobel, C.A. Bigozzi, *Coord. Chem. Rev.* 248 (2004) 1299–1316.
- [5]. M. Kapilashrami, Y. Zhang, Y.-S. Liu, A. Hagfeldt, J. Guo, *Chem. Rev.* 114 (2014) 9662–9707.
- [6]. A. Fakhruddin, R. Jose, T.M. Brown, F. Fabregat-Santiago, J. Bisquert, *Energy Environ. Sci.* 7 (2014) 3952–3981.
- [7]. B. O'Regan, M. Gratzel, *Nature* 353 (1991) 737.
- [8]. R.Koepe, N.S.Sariciftci, P.A.Troshin, R.N.L.Yubovskaya, *Applied Physics Letters* 87 (2005) 244102.
- [9]. F.Yakuphanoglu, *Solar Energy Materials&SolarCells* 91 (2007) 1182.
- [10]. Y.S. Ocak, M. A. Ebeoglu, G.Topal, T.Kılıcoglu, *Physica B* 405 (2010) 2329-2333.
- [11]. A. Tataroglu, O. Dayan, N. Ozdemir, Z. Serbetci, Ahmed A. Al-Ghamdi, A. Dere, Farid El-Tantawy, F. Yakuphanoglu, *Dyes and Pigments* 132 (2016) 64-71
- [12]. M.Soylu, I. Orak, O. Dayan, Z. Serbetci, *Microelectronics Reliability* 55 (2015) 2685-2688.
- [13]. Orak, A. Turut, M. Toprak, *Synthetic Metals* 200 (2015) 66-73.
- [14]. Ş. Aydoğan, M. Sağlam, A. Türüt, *Microelectron. Reliab.* 52 (2012) 1362-1366.
- [15]. I.H. Campbell, S. Rubin, T.A. Zawodzinski, J.D.Kress, R.L. Martin, D. L. Smith, *Phys. Rev. B* 54 (1996) 14321.
- [16]. Ö. Vural, N.Yıldırım, S.Altındal, A.Türüt, *Synth. Met* 157 (2007) 679.
- [17]. M. Soylu, *Mater. Sci. Semicond. Process.* 14 (2011) 212.
- [18]. Ö. Güllü, Ö. Barış, M. Biber, A.Türüt, *Appl. Surf. Sci.* 254 (2008) 3039.
- [19]. A.B.P. Lever, M.R. Hempstead, C.C. Leznoff, W. Lin, M. Melnik, W. A. Nevin, P. Seymour, *Pure Appl. Chem.* 58 (1986) 1467.
- [20]. J. Simon, J.J. Andre, *Molecular Semiconductors*, Springer, Berlin, 1985.
- [21]. Y. Sadaoka, T.A. Jones, W.Gopel, *Sensors Actuators B* 1 (1990) 148.
- [22]. P.F. Baude, D.A. Ender, M.A. Haase, *Appl. Phys. Lett.* 82 (2003) 3964.
- [23]. Ö. Güllü, Ş. Aydoğan, A.Türüt, *Microelectron. Eng.* 85 (2008) 1647.
- [24]. C. Temirci, M. Çakar, *Physica B* 348 (2004) 454.
- [25]. C. Özyayın, K. Akkılıç, S. İlhan, Ş. Ruzgar, Ö. Güllü, H. Temel, *Materials Science in Semiconductor Processing* 16 (2013) 1125–1130.
- [26]. W. Kern Overview and evolution of silicon wafer cleaning technology *Handbook of Silicon Wafer Cleaning Technology* (2008) 2
- [27]. O.A. Azim, M.M. Abdel-Aziz, I.S. Yahia, *Appl. Surf. Sci.* 255 (2009) 4829-4835.
- [28]. K.R. Rajesh, C.S. Menon, *The European Physical Journal B-Condensed Matter and Complex Systems* 47 (2005) 171–176.
- [29]. E. H. Rhoderick, R. H. Williams, *Metal-Semiconductor Contacts*, 2nd ed. Clarendon, Oxford, 1988.
- [30]. I. Ay, H. Tolunay, *Solid-State Electron.* 51 (2007) 381–386.
- [31]. H. Tecimer, S. Aksu, H. Uslu, Y. Atasoy, E. Bacaksız, Ş. Altındal, *Sens. Actuators* 185 (2012) 73.
- [32]. G.-F. Dalla Betta, *Advances in Photodiodes InTech*, India (2011)
- [33]. R.T. Tung *Phys. Rev. B*, 64 (2001), p. 205310

- [34]. R. Kumar, S. Chand J. Mater. Sci. Mater. Electron, 25 (2014), pp. 4531-4537
- [35]. S. K. Cheung, N. W. Cheung, Appl. Phys. Lett. 49 (1986) 85.
- [36]. J. Nelson, The Physics of Solar Cells Imperial College Press, UK (2003)
- [37]. B. Sahin, H. Cetin, E. Ayyıldız, Solid State Commun 135(2005) 490-495.
- [38]. S.M. Sze, Physics of Semiconductor Devices,(2nded) Wileyand NY,1981.
- [39]. J.P.P.R. Barry, J. Genoe, P. Heremans, Progr. Photovol. Res. Appl. 15 (2007) 659–676.
- [40]. B. Wang, H. Ding, Y. Hu, H. Zhou, S. Wang, T. Wang, et al., Int. J. Hydrogen Energy 38 (2013) 16733-16739.
- [41]. Wilmsen, C. W.,1985. Physics and Chemistry of III-V Compound Semiconductor Interfaces. Plenum Press, New York.